

Molecular Docking and ADMET Profiling of Cocoa Pod Husk Methanol-Extract Metabolites as Candidate PBP2a Inhibitors of MRSA

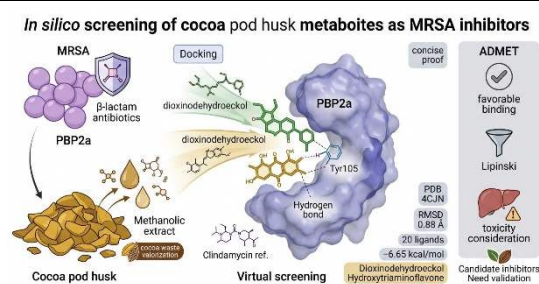
Eka Fitri Yanti^{1*}, Mohammad Rofik Usman², Cece Furwanti¹

¹Pharmacy Study Program, Sekolah Tinggi Ilmu Kesehatan Harapan Bangsa Jember, Jember, Indonesia.

²Pharmacy Study Program, Faculty of Health Sciences, Universitas dr. Soebandi, Jember, Indonesia

ABSTRACT

The incidence of *Methicillin-Resistant Staphylococcus aureus* (MRSA) resistant to β -lactam antibiotics continues to increase. MRSA resistance is primarily attributed to the presence of penicillin-binding protein 2a (PBP2a), encoded by the *mecA* gene. PBP2a is a unique membrane-associated enzyme in *S. aureus* that catalyzes the transpeptidation step in peptidoglycan biosynthesis, thereby conferring resistance to β -lactam antibiotics. Consequently, the development of novel therapeutic strategies is urgently required to combat resistant infections. An *in silico* approach utilizing cocoa pod husk (CPH) extract (*Theobroma cacao* L.) represents a promising alternative for the identification of bioactive compounds with potential anti-MRSA activity. CPH is known to contain a wide range of secondary metabolites with diverse biological properties. This study aimed to predict the PBP2a Inhibitors of compounds present in the methanolic extract of CPH using molecular docking and ADMET analysis. Molecular docking simulations were performed using AutoDock Tools, with PBP2a (PDB ID: 4CJN), retrieved from the RCSB Protein Data Bank, as the target receptor. Prior to docking, physicochemical properties of the ligands were evaluated based on Lipinski's Rule of Five (RO5) to assess drug-likeness. ADMET profiles were subsequently predicted using the pkCSM web server. The docking results demonstrated that all candidate ligands exhibited negative binding energies (< 0 kcal/mol), indicating favorable binding affinity toward PBP2a and suggesting their potential as antibacterial candidates against MRSA. ADMET prediction results revealed that the majority of metabolites in the methanolic extract of CPH possess favorable pharmacokinetic profiles.



Keywords: Molecular Docking; Cocoa Pod Husk; ADMET; PBP2a

*Corresponding Author: rofi3k4@gmail.com

How to cite: E.F. Yanti, M.R. Usman, and C. Furwanti, "Molecular Docking and ADMET Profiling of Cocoa Pod Husk Methanol-Extract Metabolites as Candidate PBP2a Inhibitors of MRSA," *Jurnal Kimia dan Pendidikan Kimia (JKPK)*, vol. 11, no. 1, pp.43-59, 2026. [Online]. Available: <https://doi.org/10.20961/jkpk.v11i1.116429>

Received: 2026-03-04

Accepted: 2026-04-22

Published: 2026-04-30

INTRODUCTION

Methicillin-Resistant *Staphylococcus aureus* (MRSA) is a isolated of *Staphylococcus aureus* exhibits resistance to β -lactam antibiotics, including methicillin, ampicillin, cephalosporins and, penicillin. MRSA has disseminated globally since the 1990s, with a continuously increasing prevalence [1]. The World Health

Organization (WHO) has categorized MRSA as a part of its priority pathogen list. Recent study by Oliván et al., approximately 15.4% of total *S. aureus* infections are attributed to MRSA, indicating a significant level of antibiotic resistance [2]. National surveillance data reported that the prevalence of MRSA infections reached 46% in 2020 and 34% in

2022, with a mortality rate of up to 63.8% [3][4].

The mechanism underlying MRSA resistance to β -lactam antibiotics involves the presence of penicillin-binding protein 2a (PBP2a), which is expressed from the *mecA* gene. PBP2a is a unique enzyme located on the *S. aureus* cell membrane that catalyzes the formation of peptidoglycan chains [5]. Unlike other PBPs, PBP2a exhibits markedly lower affinity toward β -lactam antibiotics, enabling MRSA to survive even under high concentrations of these drugs [6].

Resistant bacterial infections require novel therapeutic development and alternative approaches to combat pathogenic resistance. Cocoa pod husk (*Theobroma cacao* L.) offers a promising natural source for the discovery of antibacterial agents against MRSA through an *in silico* strategy. Cocoa pod husk (CPH), the major by-product of cocoa processing, accounts for approximately 70–75% of the total fruit weight. CPH is predominantly composed of polysaccharides, lignin, phenolics, tannins, alkaloids, and cocoa butter [7]. In other words, CPH harbors a wide range of bioactive compounds with potential biological activities [8]. Previous studies by Yahya et al. demonstrated that methanolic, ethyl acetate, and aqueous extracts of CPH effectively inhibited the growth of *S. aureus* [9].

Computational *in silico* methods represent simulation-based approaches used in the discovery of bioactive compounds with potential therapeutic activity or novel drug candidates [10]. This approach has been extensively applied for the virtual screening of natural products, as well as for elucidating the

inhibitory mechanisms of active compounds against target proteins [11][12][13]. Previous studies have shown that flavonoid compounds have strong binding affinity for PBP2a and have potential as anti-MRSA agents, which has even been validated through molecular dynamics simulations and *in vitro* assays [14]. Furthermore, another study, based on molecular docking simulation results, reported that flavonoid compounds have potential as inhibitors of the PBP2a enzyme in MRSA [15].

Procedural validation is essential in *in silico* studies to clarify ligand–receptor interactions and identify natural compounds capable of targeting specific proteins [16]. Lipinski's Rule of Five (RO5) serves as a guideline in drug discovery for predicting compounds with favorable oral bioavailability. A compound is generally considered to have good bioavailability if it meets the following criteria: LogP < 5, hydrogen bond acceptors < 10, molecular weight < 500 Da, hydrogen bond donors < 5, and molar refractivity between 40–130. However, it should be emphasized that compounds deviating from RO5 criteria are not necessarily devoid of drug-like potential [17][18].

Existing studies on natural compounds as antibacterial candidates are still largely limited to docking analysis without sufficient consideration of pharmacokinetic and toxicity aspects. Therefore, a more comprehensive approach is needed, integrating molecular docking and ADMET analysis, especially for new phytochemical sources such as metabolites from cocoa waste (cocoa pod husk), which have rarely been explored as PBP2a inhibitor candidates.

The determination of the biological activity of cocoa pod husk extracts against the bacterial protein target (PBP2a of MRSA bacteria) was conducted using molecular docking, a structure-based drug design (SBDD) method. Molecular docking is most commonly applied when the 3D structure of the target protein is available. This method aims to predict molecular recognition based on the binding affinity energy between ligands and the target protein [19]. Docking simulations were performed using AutoDock 4, employing the Lamarckian genetic algorithm to carry out molecular docking processes. Preparatory calculations were conducted using AutoGrid 4, while model preparation and docking result analysis were performed with AutoDock Tools and BioVia Discovery Studio® [20]. This study aims to explain the antibacterial potential of cocoa pod husk-derived compounds in inhibiting PBP2a protein in MRSA. In addition, Lipinski's Rule of Five was applied to predict drug-likeness for oral administration, while ADMET analysis using the pkCSM web server was performed to evaluate the pharmacokinetic properties and toxicity profiles of the compounds studied.

METHODS

The instrument used in this study is a computer equipped with an Intel i5 processor, RTX 3050 6GB GPU, and 16 GB RAM. The software utilized comprised Marvin Sketch v24.1.0, AutoDock v1.5.6, Discovery Studio Visualizer v24.1.0, Molegro Molecular Viewer (MMV) v2012.2.5, PyRx v0.9.8, RCSB Protein Data Bank, PubChem, Lipinski's Rule of Five, and pkCSM.

The materials used in this study is Twenty ligand structures in 2D, derived from metabolites of the methanolic extract were prepared for docking studies. The macromolecular structure applied in this analysis was PBP2a (PDB ID: 4CJN; pdb_00004cjn). The native ligand applied in this study was (E)-3-(2-(4-cyanostyryl)-4-oxoquinazolin-3(4H-yl)benzoic acid (QNZ)

A docking workspace folder was created to store all input files required for the docking process as well as the docking results. The receptor structure (PDB ID: 4CJN) was downloaded in 3D format from the RCSB Protein Data Bank and saved in .pdb format. The receptor and the native ligand were prepared using Molegro Molecular Viewer (MMV). The native ligand employed was (QNZ). Both receptor and ligand structures were saved in .pdb format, with removal of non-essential molecules such as water. Subsequently, hydrogen atoms were added to the receptor and ligand structures using Discovery Studio Visualizer v24.1.0.

Docking validation was performed with AutoDockTools using the native ligand. The validation was evaluated based on the Root Mean Square Deviation (RMSD) value, where $RMSD \leq 2\text{\AA}$ indicates valid docking parameters, allowing subsequent docking of test ligands [21]. In addition, the grid box was set to define the binding site of the ligands, using the native ligand as reference. The validation process was conducted with 200 runs (200 conformations).

Prior to docking, the physicochemical properties of 49 active compounds from the methanolic extract of cocoa pod husk (CPH) were predicted using the pkCSM web server.

The predicted properties included molecular weight, lipophilicity (LogP), hydrogen bond donors, hydrogen bond acceptors, and molar refractivity, based on Lipinski's Rule of Five. Compounds that complied with Lipinski's rule were downloaded in .sdf format from the PubChem database. Two-dimensional structures were prepared using MarvinSketch v24.1.0, protonated at physiological pH (7.4), and saved in.mrv format. Conformational analysis was then carried out, and the lowest-energy conformer was selected and saved in .mol2 format.

Molecular docking was carried out using AutoDockTools. Optimized receptor and ligand structures were placed in the same workspace folder. Docking was performed with grid box parameters based on the validated results, and binding affinity (free binding energy) as well as inhibition constants were recorded. The docking process was executed with 150 runs (150 conformations). Visualization of docking results was performed using Discovery Studio Visualizer. In addition, Molegro Molecular Viewer (MMV) was employed to further identify and confirm both 2D and 3D interactions between the ligands and the receptor [22].

The pharmacokinetic and toxicity (ADMET) properties of the active test compounds were predicted using the pkCSM web server. ADMET analysis included absorption (intestinal absorption and skin permeability), distribution (Volume Distribution Steady State/VDss, blood–brain barrier (BBB) penetration, and fraction unbound), metabolism (cytochrome P450 enzyme activation, particularly CYP2D6 and CYP3A4), excretion (renal and hepatic clearance of active compounds) and toxicity (including hepatotoxicity indicators).

RESULT AND DISCUSSION

Docking is a computational approach that predicts the binding mode and interactions between a ligand and its receptor [23]. Receptor preparation involves separating the protein from its native ligand to provide sufficient space for test ligands to bind to the receptor. In this study, the receptor used was the MRSA antibiotic target protein with PDB code : 4CJN, retrieved from the Protein Data Bank, with a resolution of 1.95 Å. The three-dimensional visualization of Penicillin-Binding Protein 2a (PBP2a; PDB ID: 4CJN) is presented in [Figure 1](#).

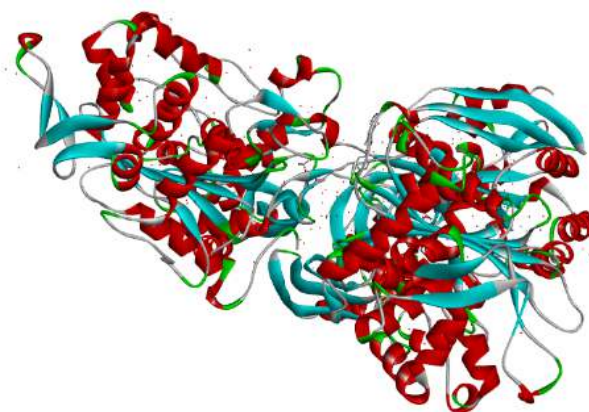


Figure 1. 3D visualization of Penicillin-Binding Protein 2a (4CJN)

The native ligand was prepared by optimizing its geometry and subjecting it to protonation at pH 7.4. Protonation was performed to ensure that the compound reflected physiological conditions in the human body. Prior to docking the test ligands against the receptor, the docking protocol must be validated (redocking) by calculating the Root Mean Square Deviation (RMSD). RMSD is a parameter used to evaluate the reliability of the docking method and to assess the extent of conformational changes in the ligand after docking. A docking protocol is considered valid if the RMSD value is $< 2 \text{ \AA}$ [24]. The smaller the RMSD value, the less structural deviation occurs, indicating that the ligand is more flexible. Flexible ligands are more likely to achieve a stable conformation upon binding to the receptor.

In this study, docking validation was carried out with 200 runs. The docking protocol produced grid box coordinates at (X: 8.054, Y: -2.917, Z: -68.370) with a box size of $40 \times 40 \times 40$ and a grid point spacing of 0.375 \AA . At the 160th run, the most stable ligand conformation was obtained, yielding an RMSD value of 0.88 \AA and a binding energy of -7.66 kcal/mol .

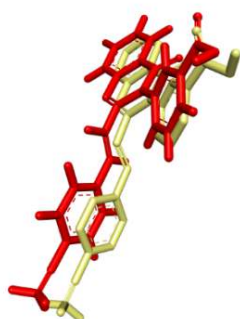


Figure 2. Superimposition of the native ligand before (red) and after redocking (yellow)

Based on the docking validation results, the parameters employed met the validity criteria, indicating that the docking protocol was reliable and could be applied to the simulation of test ligands. The test ligands used in this study were compounds identified in the methanolic extract of cocoa pod husk (CPH) as reported by Cádiz-Gurrea et al. (2020) using LC-MS analysis [25]. A total of 49 metabolites were identified in their study (Table 1) Based on Lipinski's Rule of Five (RO5) screening, 21 compounds (Tables 1 and Table 2) met the drug-likeness criteria and were subsequently selected as test ligands in this study, with clindamycin used as the positive (biological) control.

Clindamycin was selected as a positive control in this *in silico* study due to its established clinical use in the treatment of MRSA-associated infections, particularly skin and soft tissue infections [26]. Although the primary mechanism of action of clindamycin does not directly target PBP2a, its inclusion as a reference ligand in the molecular docking framework is justified by its documented clinical efficacy against certain MRSA strains [27]. Therefore, clindamycin was employed as a comparative benchmark to evaluate the binding interactions of the test ligands with the target protein, providing a relative assessment of their potential antibacterial activity. Thus, the use of clindamycin as a positive control in this study serves as a biological activity reference rather than a direct mechanistic comparator for PBP2a inhibition.

Table 1. Compounds identified in the methanolic extract of CPH with Lipinski's Rule of Five parameters

Compound	Molecular Weight	LogP	Donor acceptor	Proton donor	Molar Refractivity
Asparticacid	277.23	-2.22	6.00	2.00	65.25
Catechin(2R,3S)	290.27	1.55	6.00	5.00	74.33
Catechin(2S,3R)	290.27	1.55	6.00	5.00	74.33
Epigallocatechin(2R,3R)	306.27	1.25	7.00	6.00	76.36
Epigallocatechin(2S,3S)	306.27	1.25	7.00	6.00	76.36
Esculetin	178.14	1.20	4.00	2.00	46.53
Hexenyl	394.42	-2.38	10.00	6.00	90.44
Homovanillicacid	181.17	-0.31	4.00	1.00	44.56
Paeonol	166.18	1.60	3.00	1.00	45.15
Dioxinodehydroeckol(phlorotannin)	368.25	3.06	9.00	3.00	89.49
Protocatechuic_acid	153.11	-0.54	4.00	2.00	35.51
Quersetin_arabinofuranoside	432.34	-1.16	11.00	5.00	100.41
Theobromine	180.17	-1.04	5.00	1.00	47.14
Transclovamide	358.33	0.00	7.00	5.00	91.17
Hydroxy-triaminoflavone	283.29	1.91	6.00	4.00	83.16
N-Caffeoyl-L-aspartate	293.23	-2.51	7.00	3.00	67.27
Everlastoside_C	382.41	-2.69	10.00	6.00	86.15
Deoxyclovamide	342.33	0.29	6.00	4.00	89.15
Glucopyranoside	416.42	-2.49	10.00	6.00	96.17
Vanillic acid glucoside	329.28	-2.76	9.00	4.00	72.10
clindamycin	426.00	-1.03	6.00	5.00	112.14

Molecular docking is a computational method used to predict the interactions (binding) between small molecules and the active site of a receptor by estimating their binding energies [28]. Docking of the test ligands to the target receptor was carried out using grid box coordinates (X: 8.054, Y: -2.917, Z: -68.370), with a grid box size of 40 × 40 × 40 and a grid point spacing of 0.375 Å. The docking procedure was performed with the AutoDock software, employing the Lamarckian Genetic Algorithm (GA), and each docking run generated 150 conformations (150 runs). The selection of ligands with potential to form specific interactions with the target receptor was

based on two parameters: the binding free energy values and the types of amino acid residues involved in the interaction with the receptor [29].

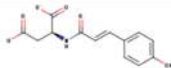
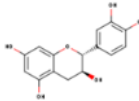
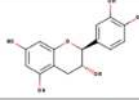
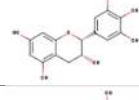

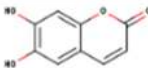
Based on the results presented in Table 3, all test ligands exhibited negative binding energy values (< 0 kcal/mol), indicating favorable interactions with the target receptor. Moreover, 19 out of 20 ligands showed lower (more negative) binding energies compared to clindamycin (positive control). Among them, dioxinodehydroeckol and hydroxytriaminoflavone exhibited the lowest binding energies at -6.65 kcal/mol. Binding energy represents the energy required for a ligand to bind to its receptor [30]. In this study,

it reflects the interaction energy between the ligands and the PBP2a receptor (PDB ID: 4CJN). Lower binding energy values indicate stronger binding affinity, which corresponds to greater stability of the ligand–receptor complex. Increased binding affinity between a compound and its target protein is often associated with enhanced potential as a therapeutic agent [31]. Therefore, based on the binding energy values, all ligands demonstrating lower binding energies than clindamycin may have potential to interact more favorably with PBP2a. However, these results should be interpreted as indicative of binding affinity rather than definitive inhibitory activity against MRSA.

Based on Table 3, four test ligands formed hydrogen bond interactions with the same amino acid residue as clindamycin. In clindamycin, hydrogen bonding occurs with the Tyr105 residue, which is similarly observed in Epigallocatechin (2S,3S), Catechin (2S,3R), Vanillic acid glucoside,

and Hexenyl. In addition, these ligands also share similarities in other interaction types with clindamycin, including alkyl, π -alkyl, sulfur–X interactions, and salt bridges involving similar amino acid residues. Active compounds are generally predicted to exhibit stronger binding when they form hydrogen bonds with the same amino acid residues or active site regions as the reference ligand. Hydrogen bonds are intermolecular interactions involving electronegative atoms (such as N, O, and F) and hydrogen atoms, arising from differences in electrostatic charge distribution. Stronger intermolecular interactions contribute to increased binding affinity, which in turn suggests a greater potential for a compound to act as a drug candidate [32]. Therefore, based on the presence of hydrogen bond interactions with the same key amino acid residue, the ligands Epigallocatechin (2S,3S), Vanillic acid glucoside, and Hexenyl are considered the most promising candidate

Table 2. Ligands and their chemical structures

Name of Ligand	Chemical structure
Ligan1_asparticacid	
Ligan2_catechin(2R,3S)	
Ligan3_catechin(2S,3R)	
Ligan4_epigallocatechin(2R,3R)	
Ligan5_epigallocatechin(2S,3S)	
Ligan6_esculetin	

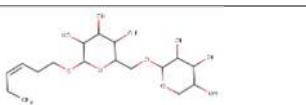
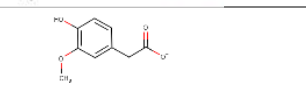
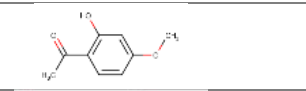
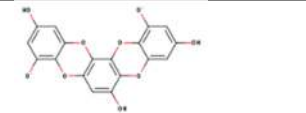
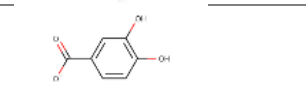
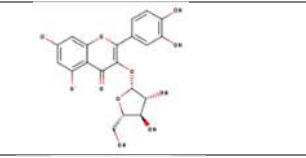
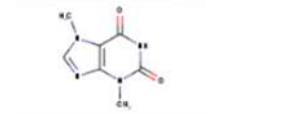
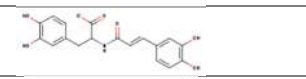
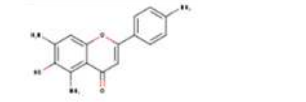
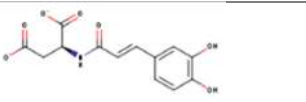
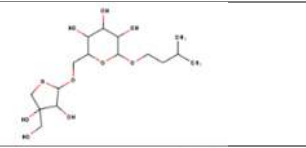
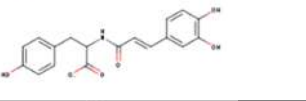
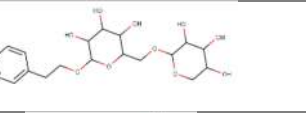
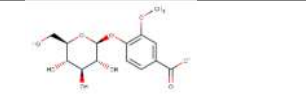
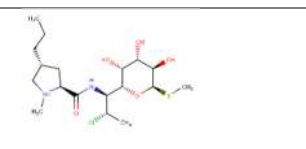
Ligan7_hexenyl	
Ligan8_homovanillicacid	
Ligan9_paeonol	
Ligan10_dioxinodehydroeckol(phlorotannin)	
Ligan11_protocatechuic_acid	
Ligan12_quersetin arabinofuranoside	
Ligan13_theobromine	
Ligan14_transclovamide	
Ligan15_hydroxy-triaminoflavone	
Ligan16_N-Caffeoyl-L-aspartate	
Ligan17_everlastoside C	
Ligan18_deoxyclovamide	
Ligan19_glucopyranoside	
Ligan20_vanillic_acid_glucoside	
Ligan21_klindamisin (control positif)	

Table 3. Docking Results of Test Ligands and Positive Control with 150 Conformations (Runs)

Ligand	Binding Energi (kcal/mol)	RMSD (Å)	Run	Hydrogen bond	Non-Hydrogen Bond Interactions
Clindamycin (kontrol positif)	-3.53	67.1	111	Tyr105	Asp295; Asp275; Ile144; Tyr297; Tyr105; Glu145
Dioxinodehydroeckol	-6.65	65.89	95	Lys316; Lys273; Glu294	Asp295
Hydroxytriaminoflavone	-6.65	60.09	143	Asp275; Glu294; Asp295; Ile144	Asn146; Glu145
Deoxyclovamide	-6.46	67.37	4	Asp275; Ile144	Asp295; Asp275; Lys316; Lys273;
Asparticacid	-6.14	66.32	100	Ile144	Lys316; Lys273
Transclovamide	-6.07	62.54	20	Ile144; Asp275	Asp295; Asp275; Lys316; Tyr105
N-caffeoyl-1-aspartate	-5.75	68.94	69	Ile144; Lys273	Lys316; Lys273
Epigallocatechin(2S3S)	-5.49	68.91	43	Tyr105; Asn146; Lys273; Asp275; Asp295	Tyr297
Homovanillicacid	-5.48	62.94	100	Asp275; Asp295; Lys316	Lys316; Lys273; Asp295
Protocatechuic acid	-5.45	66.1	41	Asn146; Asp295; Lys273	Lys316; Lys274
Catechin(2R3S)	-5.39	69.84	148	Asp295; Glu294, Lys316; Ile144	Tyr297; Tyr105; Ile144; Lys273
Quersetin arabinofuranoside	-5.37	62.36	116	Glu295; Lys273; Asp275	Tyr297
Catechin(2S3R)	-5.22	69.04	37	Lys316; Asp295; Glu294; Glu145	Arg298; Tyr297; Lys273
Vanillic acid glucoside	-5.02	69.08	81	Glu145; Arg298; Tyr105	Lys273; Lys317; Lys316; Asn146; Tyr297
Esculetin	-4.85	66.63	20	Asp295; Glu294, Lys273	
Epigallocatechin(2R3R)	-4.72	68.85	1	Ile144; Asp275; Glu294; Lys316; Asp295	Tyr297; Asn146; Lys273; Gly296
Paeonol	-4.22	66.55	84	Lys273; Lys316; Asp295	Gly296; Tyr297
Theobromine	-4.22	62.67	71	Lys316; Glu294; Asn15	Gly296; Asp295; Lys273; Tyr297
Glucopyranoside	-4.11	80.14	80	Lys316; Glu294; Asp295; Ile144	
Hexenyl	-3.72	76.9	23	Lys273; Glu294; Asp295; Ile144; Tyr105	Tyr297; Tyr105; Gly296; Asn146;

*Note: This table provides the docking outcomes for the test ligands, specifically those exhibiting lower binding energy values relative to clindamycin, which served as the reference positive control.

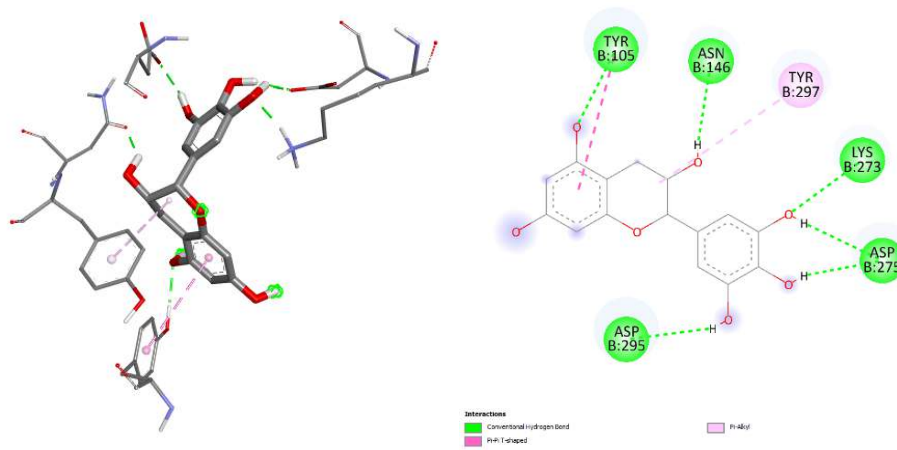


Figure 3. Three-dimensional and two-dimensional visualization of the interaction between the test ligand epigallocatechin (2S3S) and the active site of the receptor

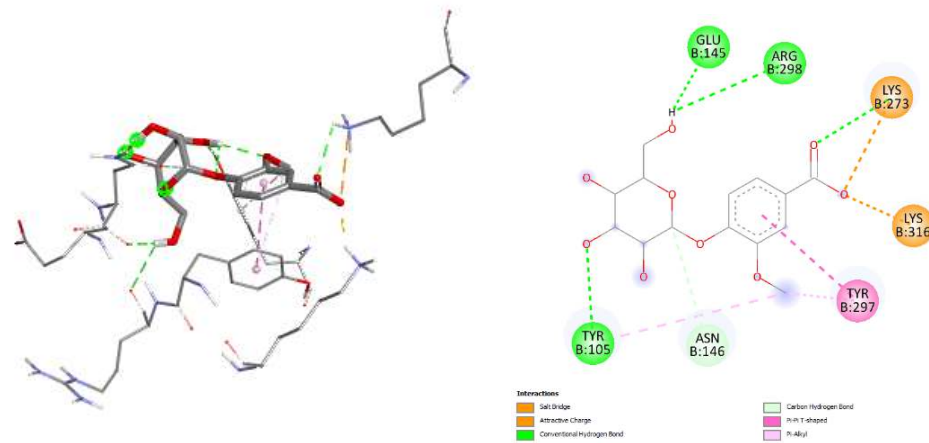


Figure 4. Three-dimensional and two-dimensional visualization of the interaction between the test ligand vanillic acid glucoside and the active site of the receptor

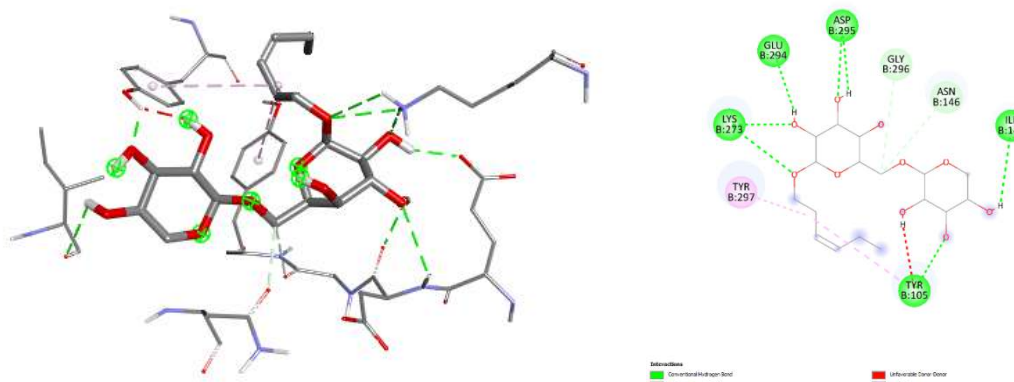


Figure 5. Three-dimensional and two-dimensional visualization of the interaction between the test ligand hexenyl and the active site of the receptor

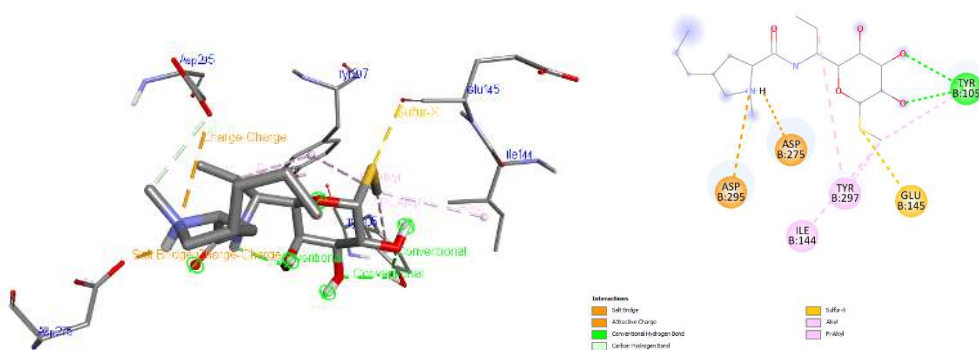


Figure 6. Three-dimensional and two-dimensional visualization of the interaction clindamicin and the active site of the receptor

Pharmacokinetic and toxicity (ADMET) data were obtained from the pkCSM web server, as presented in Table 4. Pharmacokinetics begins with drug absorption, which refers to the transfer of a drug from its site of administration into the bloodstream. A critical step in this process is intestinal absorption, which denotes the uptake of a compound through the intestinal lining into systemic circulation. A drug is considered to have good intestinal absorption if its absorption rate exceeds 30% [33]. In this study, three compounds—hexenyl, N-caffeoyl-L-aspartate, and vanillic acid glucoside—did not meet this criterion, suggesting that they are unlikely to be efficiently absorbed via the intestinal tract. Additionally, transdermal drug delivery, evaluated via skin permeability values, revealed that only one compound, paeonol, failed to meet the requirement. A compound is considered to have favorable skin permeability if the $\log K_p$ value is greater than -2.5 [33]. Therefore, compounds with $\log K_p$ values below -2.5 are predicted to be unsuitable for transdermal absorption.

Drug distribution represents the movement of a compound from systemic

circulation to various tissues and organs. In this study, drug distribution was evaluated based on Volume Distribution steady state (VDss), Blood-Brain Barrier permeability (BBB), and Fraction unbound. The VDss reflects the tendency of a drug to remain in plasma. A compound is considered to meet the criterion if $\log VD < -0.15$ and is classified as highly favorable when the $\log VD > 0.45$ [31]. According to Table 4, eight active compounds fulfilled this requirement: catechin (2R,3S), catechin (2S,3R), epigallocatechin (2R,3R), epigallocatechin (2S,3S), hexenyl, paeonol, quercetin arabinofuranoside, and glucopyranoside. However, none of these eight compounds demonstrated very high values, defined as $\log VD > 0.45$.

The predicted blood–brain barrier (BBB) permeability values for all active compounds were very low, with some values even below -1 . This suggests that the compounds are unlikely to cross the BBB and therefore are predicted to have minimal central nervous system (CNS) side effects or toxicity. Compounds with BBB permeability values > 0.3 are generally considered capable of penetrating the BBB and may

pose a higher risk of CNS-related adverse effects [33]. Regarding the unbound fraction, all active compounds met the acceptable criteria. The unbound fraction is used to estimate the extent of a compound's binding to plasma proteins. A higher unbound fraction indicates a greater proportion of free (unbound) drug in circulation, which may enhance its availability to interact with the target receptor. However, this parameter primarily reflects plasma protein binding rather than direct binding affinity to the target protein [33].

In the pharmacokinetic process, drug distribution is subsequently followed by metabolic processes. Metabolic reactions primarily occur through oxidative processes in the body, particularly in the liver. The metabolic profile of the active compounds was predicted using cytochrome P450 (CYP) inhibition parameters (Table 4). The enzymes evaluated in this study were CYP2D6 and CYP3A4, both of which are major cytochrome P450 isoforms involved in the metabolism of a wide range of drugs. Inhibition of these enzymes may lead to drug–drug interactions, potentially reducing therapeutic efficacy [34, 35]. Based on the data presented in Table 4, all active compounds from the methanolic extract of CPH were predicted to neither inhibit nor induce CYP2D6. However, hydroxy-triaminoflavone was predicted to inhibit CYP3A4. Such inhibitory activity may interfere with normal drug metabolism, leading to increased plasma drug concentrations. Elevated drug levels in the bloodstream may result in adverse effects and, in severe cases, may lead to toxic or even fatal outcomes [35, 36].

Following metabolism, drugs are subsequently eliminated from the body through excretion. In this study, excretory properties were evaluated based on Total Clearance and Renal Organic Cation Transporter 2 (OCT2) parameters. OCT2 is a renal transporter that plays a critical role in drug disposition and clearance processes, while total clearance reflects the overall rate at which a compound is eliminated from the body. As shown in Table 4, the total clearance values of the active compounds from the methanolic extract of CPH ranged from 0.24 to 1.70, suggesting their predicted excretion rates. Higher total clearance values indicate faster elimination of compounds from the body [37]. In this investigation, two compounds, namely hexenyl and glucopyranoside, exhibited higher total clearance values than clindamycin. However, none of the 19 active compounds were predicted to act as OCT2 substrates or inhibitors.

Toxicity is also a crucial parameter in drug development because it determines the safety profile and feasibility of a compound as a potential therapeutic agent. In this study, toxicity was evaluated based on hepatotoxicity predictions using pkCSM analysis. Theobromine, vanillic acid glucoside, and clindamycin were predicted to exhibit hepatotoxic effects. These findings suggest that these compounds may require further safety evaluation before being considered as drug candidates. Hepatotoxicity is particularly important because the liver plays a central role in drug metabolism and is highly susceptible to chemical-induced injury. These toxic effects

are associated with the induction of reactive oxygen species (ROS) formation and subsequent mitochondrial damage in hepatocytes [38]. Therefore, although several active compounds from the

methanolic extract of CPH showed favorable pharmacokinetic properties, their potential hepatotoxicity should be carefully considered in further in vitro and in vivo studies.

Table 4. Predicted pharmacokinetic (absorption, distribution, metabolism, excretion) and toxicity (ADMET) profiles of active compounds from the CPH extract. Data were obtained from the pkCSM web server.

Ligand	Absorption		Distribution			Metabolism		Excretion		Toxicity
	Intestinal absorption	Skin Permeability	VD _{ss}	Fraction unbound	BBB permeability	CYP2D6 inhibitor	CYP3A4 inhibitor	Total Clearance	Renal OCT2	Hepatotoxicity
Aspartic acid	24.71	-2.74	-1.64	0.419	-0.658	No	No	0.615	No	No
Catechin(2R,3S)	72.36	-2.74	0.259	0.181	-1.20	No	No	0.29	No	No
Catechin(2S,3R)	72.36	-2.74	0.259	0.181	-1.20	No	No	0.29	No	No
Epigallocatechin(2R,3R)	65.10	-2.74	0.23	0.167	-1.51	No	No	0.45	No	No
Epigallocatechin(2S,3S)	65.10	-2.74	0.23	0.167	-1.51	No	No	0.45	No	No
Esculetin	65.76	-2.73	-0.26	0.418	-0.14	No	No	0.74	No	No
Hexenyl	20.33	-2.74	0.35	0.574	-1.13	No	No	1.70	No	No
Homovanillic acid	76.15	-2.74	-1.19	0.504	0.00	No	No	0.47	No	No
Paeonol	94.23	-2.21	-0.07	0.433	0.04	No	No	0.67	No	No
Dioxinodihydroxyflavone(phlorotannin)	98.24	-2.74	-1.02	0.159	-1.15	No	No	0.54	No	No
Protocatechuic acid	65.88	-2.74	-2.08	0.547	-0.08	No	No	0.62	No	No
Quercetin arabinofuranoside	56.48	-2.74	0.00	0.164	-1.30	No	No	0.27	No	No
Theobromine	98.38	-2.76	-0.15	0.729	-0.38	No	No	0.34	No	Yes
Transclovamide	45.86	-2.74	-0.58	0.147	-1.04	No	No	0.29	No	No
Hydroxytriaminoflavone	77.94	-2.74	-0.25	0.158	-1.01	No	Yes	0.24	No	No
N-Caffeoyl-L-aspartate	21.61	-2.74	-1.35	0	-0.66	No	No	0.59	No	No
Deoxyclovidin	46.52	-2.74	-1.27	0.108	-0.85	No	No	0.31	No	No
Glucopyranoside	33.27	-2.74	0.08	0.552	-0.87	No	No	1.20	No	No
Vanillic acid glucoside	19.77	-2.74	-1.20	0.467	-1.12	No	No	0.75	No	Yes
clindamicin	53.28	-2.90	-0.21	0.75	-0.94	No	No	0.82	No	Yes

CONCLUSION

Based on the results of Lipinski's Rule of Five (RO5) analysis, ADMET prediction, and molecular docking using a validated grid box, a total of 20 metabolites from the methanolic extract of cocoa pod husk (CPH) and one compound as a positive control were evaluated. All compounds exhibited negative binding energy values (< 0 kcal/mol), indicating their potential as candidate inhibitors of PBP2a, the target protein associated with MRSA. Among the tested compounds, dioxinodehydroeckol and hydroxytriaminoflavone demonstrated the lowest binding energies (-6.65 kcal/mol), which were even lower than that of the positive control. In terms of interaction profiles, Epigallocatechin (2S,3S), Catechin (2S,3R), Vanillic acid glucoside, and Hexenyl formed hydrogen bond interactions with the Tyr105 residue, which is also involved in the binding of the reference ligand.

ADMET predictions using the pkCSM platform revealed that the majority of metabolites in the methanolic extract of CPH possess favorable pharmacokinetic properties, including acceptable absorption, distribution, metabolism, and excretion profiles. However, some compounds exhibited limitations in intestinal absorption, skin permeability, and potential inhibition of CYP enzymes. Furthermore, most compounds were predicted to be relatively safe in terms of toxicity, although certain metabolites showed potential hepatotoxicity, which should be carefully considered in further drug development as candidate therapeutics. Further studies can be conducted with further in silico testing such

as molecular dynamics, enzyme inhibition assays, and microbiological assays both in vitro and in vivo.

ACKNOWLEDGEMENT

The authors would like to express their gratitude to KEMDIKTISAINTEK through the Direktorat Penelitian Pengabdian Masyarakat (DPPM) for the research grant under Penelitian Dosen Pemula (0419/C3/DT.05.00/2025).

REFERENCES

- [1] Xing, A., et al., *The Prevalence, Epidemiological, and Molecular Characterization of Methicillin-Resistant Staphylococcus aureus (MRSA) in Macau (2017–2022)*. *Microorganisms*, 2024. 12(1): p. 148. <https://doi.org/10.3390/microorganisms12010148>
- [2] Oliván, P.M., et al., *Prevalence and risk factors for methicillin-resistant Staphylococcus aureus infection in children*. national center for Biotechnology Information, 2024. 37(2): p. 170-175. <https://doi.org/10.37201/req/113.2023>
- [3] D. Anggraini et al., "Antibiotic resistance report from the Surveillance of Indonesia Network on Antimicrobial Resistance (SINAR) 2023," *Journal of Global Antimicrobial Resistance*, vol. 39, p. 20, 2024, doi: [10.1016/j.jgar.2024.10.061](https://doi.org/10.1016/j.jgar.2024.10.061).
- [4] Hoste, S.I.B.K.H.V.E.A. and F.A. Colardyn, *Outcome and attributable mortality in critically ill patients with bacteremia involving methicillin-susceptible and methicillin-resistant Staphylococcus aureus*. *JAMA Internal Medicine*, 2002. 162(19). <https://doi.org/10.1001/archinte.162.19.2229>
- [5] Tang, S.S., A. Apisarnthanarak, and L.Y. Hsu, *Mechanisms of β -lactam*

- antimicrobial resistance and epidemiology of major community- and healthcare-associated multidrug-resistant bacteria.* Adv Drug Deliv Rev, 2014. 78: p. 3-13. <https://doi.org/10.1016/j.addr.2014.08.003>
- [6] Hartman, B. and A. Tomasz, *Altered penicillin-binding proteins in methicillin-resistant strains of staphylococcus aureus.* Antimicrob Agents Chemother, 1981. 19(5): p. 726-735. <https://doi.org/10.1128/AAC.19.5.726>
- [7] Jusmiati, J., R. Rusli, and L. Rijai, *Aktivitas Antioksidan Kulit Buah Kakao Masak dan Kulit Buah Kakao Muda.* Jurnal Sains dan Kesehatan, 2015. 1(1): p. 34-39. <https://orcid.org/0000-0002-1087-1112>
- [8] Campos-Vega, R., K.H. Nieto-Figueroa, and B.D. Oomah, *Cocoa (Theobroma cacao L.) pod husk: Renewable source of bioactive compounds.* Trends in Food Science & Technology, 2018. 81: p. 172-184. [10.1016/j.tifs.2018.09.022](https://doi.org/10.1016/j.tifs.2018.09.022)
- [9] Yahya, M., B. Ginting, and N. Saidi, *In-Vitro Screenings for Biological and Antioxidant Activities of Water Extract from Theobroma cacao L. Pod Husk: Potential Utilization in Foods.* molecules, 2021. 26(22). [10.3390/molecules26226915](https://doi.org/10.3390/molecules26226915)
- [10] Pelkonen, O., M. Turpeinen, and H. Raunio, *In vivo-in vitro-in silico pharmacokinetic modelling in drug development: current status and future directions.* Clin Pharmacokinet, 2011. 50(8): p. 483-491. [10.2165/11592400-000000000-00000](https://doi.org/10.2165/11592400-000000000-00000)
- [11] A. Hardianto M. Yusuf, M., F. Liu, and S. Ranganathan, *Structure-Based Drug Design Workflow.* Encyclopedia of Bioinformatics and Computational Biology, 2019. 3: p. 273-282.
- [12] Hardianto, A., et al., *Exploring the Potency of Nigella sativa Seed in Inhibiting SARS-CoV-2 Main Protease Using Molecular Docking and Molecular Dynamics Simulations.* Indonesian Journal of Chemistry, 2021. 21(5): p. 1252-1262. [10.22146/ijc.65951](https://doi.org/10.22146/ijc.65951)
- [13] M. Yusuf, M., et al., *Introduction of Docking-Based Virtual Screening Workflow Using Desktop Personal Computer.* Encyclopedia of Bioinformatics and Computational Biology, 2019. 9: p. [10.1016/B978-0-12-809633-8.20277-X](https://doi.org/10.1016/B978-0-12-809633-8.20277-X)
- [14] Alhadrami, H. A., *Flavonoids as Potential anti-MRSA Agents through Modulation of PBP2a: A Computational and Experimental Study.* Antibiotics, 2020. 9(9): p. [10.3390/antibiotics9090562](https://doi.org/10.3390/antibiotics9090562)
- [15] Verma, A. K., et al., *Molecular docking and simulation studies of flavonoid compounds against PBP-2a of methicillin-resistant Staphylococcus aureus.* J Biomol Struct Dyn, 2022. 40 (21): p. [10.1080/07391102.2021.1944911](https://doi.org/10.1080/07391102.2021.1944911)
- [16] Hardianto, A., et al., *Structure-Based Drug Design Workflow.* Elsevier, 2019. 3: p. 273-282. [10.1016/B978-0-12-809633-8.20104-0](https://doi.org/10.1016/B978-0-12-809633-8.20104-0)
- [17] Yang, W., et al., *The Evolving Druggability and Developability Space: Chemically Modified New Modalities and Emerging Small Molecules.* AAPS J, 2020. 22(2): p. 21. [10.1208/s12248-019-0402-2](https://doi.org/10.1208/s12248-019-0402-2)
- [18] Lipinski, C.A., et al., *Experimental and computational approaches to estimate solubility and permeability in drug discovery and development settings.* Adv Drug Deliv Rev, 2001. 4(1-3): p. 3-26. [10.1016/S0169-409X\(00\)00129-0](https://doi.org/10.1016/S0169-409X(00)00129-0)
- [19] Stanzione, F., I. Giangreco, and J.C. Cole, *Use of molecular docking computational tools in drug discovery.* Prog Med Chem, 2021. 60: p. 273-343. [10.1016/bs.pmch.2021.01.004](https://doi.org/10.1016/bs.pmch.2021.01.004)

- [20] Sabe, V.T., et al., *Current trends in computer aided drug design and a highlight of drugs discovered via computational techniques: A review*. Eur J Med Chem, 2021. 15: p. 224. [10.1016/j.ejmech.2021.113705](https://doi.org/10.1016/j.ejmech.2021.113705)
- [21] Muttaqin, F.Z., M.F. Pratama, and F. Kurniawan, *Molecular Docking and Molecular Dynamic Studies of Stilbene Derivative Compounds as Sirtuin-3 (Sirt3) Histone Deacetylase Inhibitor on Melanoma Skin Cancer and Their Toxicities Prediction*. Journal of Pharmacopolium, 2019. 2(2): p. 112-121. <https://doi.org/10.36465/jop.v2i2.489>
- [22] Mardianingrum, R., et al., *Studi in silico senyawa 1, 4-Naphthalenedione-2-Ethyl-3-Hydroxy sebagai antiinflamasi dan antikanker payudara*. ALCHEMY Jurnal Penelitian Kimia, 2021. 17(1): p. 83-95. [10.20961/alchemy.17.1.43979.83-95](https://doi.org/10.20961/alchemy.17.1.43979.83-95)
- [23] Girija, C.R., et al., *Molecular Docking Studies of Curcumin Derivatives with Multiple Protein Targets for Procarcinogen Activating Enzyme Inhibition*. Journal of Proteomics & Bioinformatics, 2010. 3(6): p. 200-203. [10.4172/jpb.1000140](https://doi.org/10.4172/jpb.1000140)
- [24] Cole, J.C., et al., *Comparing protein-ligand docking programs is difficult*. Proteins, 2005. 60(3): p. 325-332. [10.1002/prot.20497](https://doi.org/10.1002/prot.20497)
- [25] Cádiz-Gurrea, M.d.I.L., et al., *LC-MS and Spectrophotometric Approaches for Evaluation of Bioactive Compounds from Peru Cocoa By-Products for Commercial Applications*. molecules, 2020. 25(3177): p. 1-16. [10.3390/molecules25143177](https://doi.org/10.3390/molecules25143177)
- [26] Stevens, D.L., et al., *Practice guidelines for the diagnosis and management of skin and soft tissue infections*. Clinical Infectious Diseases, 2014. 59(2): p. 10-52. [10.1093/cid/ciu296](https://doi.org/10.1093/cid/ciu296)
- [27] Daum, R.S., *Clinical practice. Skin and soft-tissue infections caused by methicillin-resistant Staphylococcus aureus*. New England Journal of Medicine, 2007. 357(4). [10.1056/NEJMcp070747](https://doi.org/10.1056/NEJMcp070747)
- [28] Guedes, I.A., C.S.d. Magalhães, and L.E. Dardenne, *Receptor-Ligand Molecular Docking*. Biophys Rev, 2013. 6(1): p. 75-87. [10.1007/s12551-013-0130-2](https://doi.org/10.1007/s12551-013-0130-2)
- [29] Oliveira, T.A.d., et al., *Evaluation of Docking Machine Learning and Molecular Dynamics Methodologies for DNA-Ligand Systems*. Pharmaceuticals, 2022. 15(2): p. 132. [10.3390/ph15020132](https://doi.org/10.3390/ph15020132)
- [30] Aziz, F.K., et al., *Hasil in Silico Senyawa Z12501572, Z00321025, SCB5631028 dan SCB13970547 Dibandingkan Turunan Zerumbon Terhadap Human Liver Glycogen Phosphorylase (115Q) Sebagai Antidiabetes*. Jurnal Kimia Valensi, 2016. 2(2): p. 120-124. [10.15408/jkv.v2i2.4170](https://doi.org/10.15408/jkv.v2i2.4170)
- [31] Du, X., et al., *Insights into Protein-Ligand Interactions: Mechanisms, Models, and Methods*. Int. J. Mol. Sci, 2016. 17(2): p. 144. [10.3390/ijms17020144](https://doi.org/10.3390/ijms17020144)
- [32] Liu, J., L. Fang, and C. Liu, *Investigating the influences of intermolecular interactions on viscoelastic performance of pressure-sensitive adhesive by FT-IR spectroscopy and molecular modeling*. Drug Development and Industrial Pharmacy, 2020. 46(6). [10.1080/03639045.2020.1764026](https://doi.org/10.1080/03639045.2020.1764026)
- [33] Pires, D.E.V., T.L. Blundell, and D.B. Ascher, *pkCSM: Predicting Small-Molecule Pharmacokinetic and Toxicity Properties Using Graph-Based Signatures*. Journal of Medicinal Chemistry, 2015. 58(9): p. 4066-4072. [10.1021/acs.jmedchem.5b00104](https://doi.org/10.1021/acs.jmedchem.5b00104)
- [34] Brignac-Huber, L.M., et al., *Relationship Between CYP1A2 Localization and Lipid Microdomain*

- Formation as a Function of Lipid Composition*. Drug metabolism and disposition, 2013. 4(11): p. 1896-1905. [10.1124/dmd.113.053611](https://doi.org/10.1124/dmd.113.053611)
- [35] Ashour, M.L., et al., *Inhibition of Cytochrome P450 (CYP3A4) Activity by Extracts from 57 Plants Used in Traditional Chinese Medicine (TCM)*. Pharmacognosy magazine, 2017. 13(50): p. 300-308. [10.4103/0973-1296.204561](https://doi.org/10.4103/0973-1296.204561)
- [36] Sari, N.E., et al., *Potensi Interaksi Obat-Obat yang Dimediasi Sitokrom P450 pada Pasien Geriatri di Rawat Inap Rumah Sakit X*. Health Information : Jurnal Penelitian, 2023. 15(2). [10.1002/prp2.210](https://doi.org/10.1002/prp2.210)
- [37] Li, Y., et al., *Slow drug delivery decreased total body clearance and altered bioavailability of immediate and controlled-release oxycodone formulations*. Pharmacology research & Perspectives, 2016. 4(1): p. 1-13. <https://doi.org/10.1002/prp2.210>
- [38] Yuan, L. and N. Kaplowitz, *Mechanisms of Drug-Induced Liver Injury*. Clin Liver Dis., 2013. 17(4): p. 507-518. [10.1016/j.cld.2013.07.002](https://doi.org/10.1016/j.cld.2013.07.002)